Lower blood glucose, hyperglucagonemia, and pancreatic α cell hyperplasia in glucagon receptor knockout mice

R. W. Gelling*†, X. Q. Du†, D. S. Dichmann‡, J. Rømer*, H. Huang†, L. Cui†, S. Obici§, B. Tang¶, J. J. Holst‖, C. Fledelius**, P. B. Johansen††, L. Rossetti§, L. A. Jelicks¶, P. Serup‡, E. Nishimura‡‡, and M. J. Charron†§§

Departments of ‡‡Diabetes Biology, *Pharmacological Research 4, **Pharmacological Research 2, and ††Pharmacological Research 3, Novo Nordisk A/S, DK-2880 Bagsvaerd, Denmark; Departments of †Biochemistry, §Medicine (Endocrinology), and ¶Physiology and Biophysics, Albert Einstein College of Medicine, Bronx, NY 10461; ‡Department of Developmental Biology, Hagedorn Research Institute, DK-2820 Gentofte, Denmark; and ‖Department of Medical Physiology, Panum Institute, DK-2200 Copenhagen, Denmark

Communicated by Bruce S. McEwen, The Rockefeller University, New York, NY, November 21, 2002 (received for review February 21, 2002)

Glucagon, the counter-regulatory hormone to insulin, is secreted from pancreatic α cells in response to low blood glucose. To examine the role of glucagon in glucose homeostasis, mice were generated with a null mutation of the glucagon receptor (Gcgr$^{-/-}$). These mice display lower blood glucose levels throughout the day and improved glucose tolerance but similar insulin levels compared with control animals. Gcgr$^{-/-}$ mice displayed supraphysiological glucagon levels associated with postnatal enlargement of the pancreas and hyperplasia of islets due predominantly to α cell, and to a lesser extent, δ cell proliferation. In addition, increased proglucagon expression and processing resulted in increased pancreatic glucogen-like peptide 1 (GLP-1) (1–37) and GLP-1 amide (1–36 amide) content and a 3- to 10-fold increase in circulating GLP-1 amide. Gcgr$^{-/-}$ mice also displayed reduced adiposity and leptin levels but normal body weight, food intake, and energy expenditure. These data indicate that glucagon is essential for maintenance of normal glycemia and postnatal regulation of islet and α and δ cell numbers. Furthermore, the lean phenotype of Gcgr$^{-/-}$ mice suggests glucagon action may be involved in the regulation of whole body composition.

Glucagon is a 29-aa pancreatic hormone derived from tissue-specific processing of proglucagon such that glucagon and the major proglucagon fragment are the primary products in α cells of the islets of Langerhans, and glucagon-like peptide-1 (GLP-1), oxyntomodulin, and glicentin are produced by the intestinal L cells and central nervous system (CNS) (1, 2). Glucagon is secreted from the pancreatic α cells into the portal blood supply in response to hypoglycemia and acts as the counterregulatory hormone to insulin. The main action of glucagon is to stimulate hepatic glucose production (HGP) by increasing glycogenolysis and gluconeogenesis while inhibiting glycogen synthesis. In addition, glucagon has many extrahepatic effects, including positive inotropic effects in the heart, increased lipolysis in adipose tissue, action as a satiety factor in the CNS, regulatory effects on glomerular filtration rate, and intraislet regulation of insulin, glucagon, and somatostatin secretion (1–4). In contrast, nutrient-stimulated release of GLP-1 from the intestine acts in a glucose-dependent manner to stimulate insulin secretion, inhibit glucagon secretion, and stimulate insulin biosynthesis and islet proliferation (3, 5, 6). In addition, GLP-1 has a number of extrapancreatic effects, including inhibition of gastric emptying and food intake, regulation of hypothalamic–pituitary function, and involvement in the CNS aversion response (6).

The wide range of actions of glucagon is correlated to the equally wide tissue distribution of its specific receptor (Gcgr), which has been cloned from rat (7), human (8), and mouse (9). Sequence homology analysis indicates that the Gcgr is a member of the class B family of heptahelical GTP-binding protein (G protein) coupled receptors, which includes those for the related peptides GLP-1 and glucose-dependent insulinotropic polypeptide (10). In the current study, mice with a targeted deletion within the glucagon receptor gene (Gcgr$^{-/-}$) were generated to more fully investigate the role of glucagon in glucose homeostasis.

Methods

Strategy for *Gcgr* Gene Disruption. A 10.5-kb *Hin*dIII/EcoRI fragment of the murine *Gcgr* gene (9) was used to construct the targeting vector (Fig. 6 *A* and *B*, which is published as supporting information on the PNAS web site, www.pnas.org). Exons 3–6 were replaced with a phosphoglyceate kinase promoted neomycin resistance cassette, and the negative selectable thymidine kinase gene was engineered into the 3′ and 5′ ends. SfiI linearized plasmid (25 μg) was electroporated into WW6 embryonic stem cells ($\approx 5 \times 10^6$ cells), as described (11). Positive targeting of the mutant allele was confirmed by Southern (Fig. 6*B*) and/or PCR analysis (data not shown).

Animals. Animals were fed ad libitum unless otherwise noted and maintained in a murine hepatitis virus-free barrier facility on a 12-h light/12-h dark cycle. Mice backcrossed (F_6 and F_7) onto the C57/BL6J background and littermate controls were studied, and major findings were confirmed in males and females (see Figs. 7 and 8, which are published as supporting information on the PNAS web site) from two independent lines. All data presented are from male mice unless otherwise noted. All protocols were approved by the institutional Animal Care and Use Committees.

Liver and Epididymal Fat Pad Measurements. Liver plasma membrane preparations (12), binding studies (13), hormone-stimulated cAMP accumulation (13), and determination of glycogen levels (14, 15) were as previously described. White adipose tissue (WAT) lipolysis was measured as in ref. 16.

Intraperitoneal Glucose Tolerance Test (IPGTT), Glucagon Challenge (GC), and Insulin Tolerance Test (ITT). After a 12- to 16-h (IPGTT) and 6-h (GC and ITT) fasting period, conscious mice were i.p. administered either a glucose load of 1.5 g/kg, 16 μg/kg human glucagon, or 0.75 units/kg porcine insulin. Tail blood was taken at the times indicated and glucose levels determined by using a OneTouch II glucose meter (LifeScan, Milpitas, CA).

Plasma Metabolites and Hormones. Plasma was obtained from retroorbital blood spun at 5,000 $\times$ *g*. Lactate and free fatty acids

Abbreviations: Gcgr, glucagon receptor; GLP-1, glucagon-like peptide-1; BG, blood glucose; IPGTT, i.p. glucose tolerance test; ITT, insulin tolerance test; HGP, hepatic glucose production; WAT, white adipose tissue.

§§To whom correspondence should be addressed. E-mail: charron@aecom.yu.edu.

www.pnas.org/cgi/doi/10.1073/pnas.0237106100

were measured by using kits from Sigma and Wako Chemicals (Neuss, Germany), respectively. Clinical chemistries were run on a Synchron CX5 Autoanalyzer (Beckman Instruments, High Wycombe, U.K.). Triglycerides, glucose, cholesterol, and high density lipoprotein were determined by using standard human kits. Low density lipoprotein was analyzed by a user-defined method (Diagnostic Chemicals, Charlottetown, Canada). Insulin and leptin levels were determined with murine ELISAs (Crystal Chem, Chicago). Glucagon, corticosterone, insulin-like growth factor-1, and epinephrine were determined with RIAs from Linco Research Immunoassay (St. Charles, MO), DPC (Los Angeles), Mediagnostics (Hamburg, Germany), and DLD Diagnostika (Adlerhorst, Germany), respectively.

Pancreatic Hormone Extraction. After cervical dislocation, the pancreas was quickly freeze-clamped in liquid nitrogen and stored at −80°C until processed. Tissues were weighed and then homogenized twice in 2.5 ml of 0.5% trifluoroacetic acid by using a glass/glass homogenizer and left for 1 hr at 4°C. Samples were rehomogenized, spun at 10,000 × *g*, and supernatants were stored at −20°C. Before analysis, extracts were purified on SepPak C18 (Waters) cartridges (17). Hormone concentrations were determined by using established RIAs with antibodies specific for either the central region of GLP-1 (total GLP-1) or the amidated C terminus, which have been described (17).

Food Intake and Body Weight. Cumulative food intake and body weight were measured once per week in group-housed mice (four mice per cage) for 19 wk. In addition, food intake was accessed in individually housed mice, as described below.

Indirect Calorimetry. Mice were individually housed and acclimated to the calorimeter cages for 1 day before 2–3 days of data collection of gas exchanges and food intake. Indirect calorimetry was performed with a computer-controlled open circuit calorimetry system (Oxymax, Columbus Instruments, Columbus, OH) comprised of four respiratory chambers equipped with a stainless steel elevated wire floor, water bottle, and food tray connected to a balance. Oxygen consumption and CO_2 production were measured for each mouse at 6-min intervals, and outdoor air reference values were determined after every 10 measurements. Instrument settings were: gas flow rate = 0.5 liters/min; settle time = 240 sec; measure time = 60 sec. Gas sensors were calibrated daily with primary gas standards containing known concentrations of O_2, CO_2, and N_2 (Tech Air, White Plains, NY). A mass flow meter was used to measure and control air flow. Oxygen was measured by an electrochemical sensor based on limited-diffusion metal air battery. CO_2 was measured with a spectrophotometric sensor. Respiratory quotient was calculated as the ratio between CO_2 production (liters) over O_2 consumption (liters). Energy expenditure was calculated by the equation: $EE = (3.815 + 1.232 \times VCO_2/VO_2) \times VO_2$.

MRI Analysis. MRI data were acquired by using a GE Omega 400WB spectrometer (General Electric). Anesthetized mice were placed in the MRI coil, and proton spectra and images were acquired. Fat mass was calculated as described by Stein *et al*. (18). Fat content was analyzed by a thresholding method based on histogram analysis of the region of interest.

Antisera and Immunohistochemistry. Guinea pig antiinsulin and mouse monoclonal antiglucagon Glu-001 and antisomatostatin were obtained from Novo Nordisk A/S (Bagsvaerd, Denmark) or ICN and described previously (19). Immunohistochemistry and image processing were performed as described (20). The secondary antibodies fluorescein isothiocyanate−, Cy-2−, and Texas red-conjugated were from Jackson ImmunoResearch,

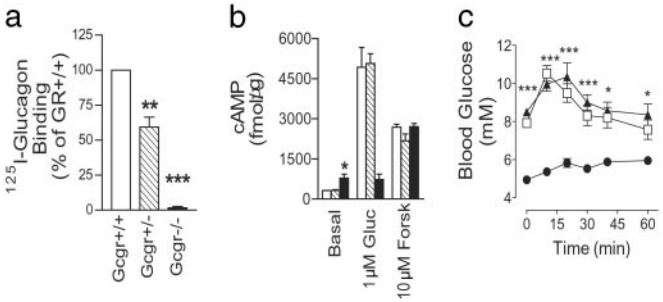

Fig. 1. Gcgr$^{-/-}$ mice lack functional glucagon receptors. [^{125}I]Glucagon-binding (*a*) and glucagon-stimulated cAMP production (*b*) in liver membranes from male Gcgr$^{+/+}$, Gcgr$^{+/-}$, and Gcgr$^{-/-}$ mice. Control (open bars), Gcgr$^{+/-}$ (hatched bars), and Gcgr$^{-/-}$ (filled bars) mice are indicated. Gluc, glucagon; Forsk, forskolin. Data represent mean ± SEM ($n = 3$) from three independent preparations. (*c*) Intraperitoneal glucagon challenge of male Gcgr$^{-/-}$ (●), Gcgr$^{+/-}$ (▲), and Gcgr$^{+/+}$ (□) mice. Data represent mean ± SEM, $n = 5$–7. *, $P < 0.05$; **, $P < 0.01$; ***, $P < 0.001$.

goat anti-mouse Alexa 546 was from Molecular Probes, and rabbit anti-guinea pig FITC was from DAKO.

Statistical Analyses. Data are mean ± SEM. Statistical significance was determined by ANOVA by using Bonferroni's multiple comparisons post hoc test when appropriate. Unpaired two-tailed Student's *t* test was applied to all other statistical analyses.

Results

Targeting the Gcgr Locus. A gene targeting strategy was used to delete exons 3–6 of the murine *Gcgr* gene by homologous recombination (Fig. 6*A*). Of three targeted embryonic stem cell clones, two independent germline transmitting male chimeras were obtained. Heterozygous (Gcgr$^{+/-}$) matings yielded null (Gcgr$^{-/-}$) mice at a Mendelian ratio that were identified by Southern blot (Fig. 6*B*) and/or PCR analysis (data not shown). Gcgr$^{-/-}$ mice displayed normal growth rates (Fig. 8, which is published as supporting information on the PNAS web site). Although Gcgr$^{-/-}$ male mice are fertile, Gcgr$^{-/-}$ females were poor breeders, giving birth to small litters, which were often stillborn or died shortly after birth. The cause of this reproductive success may be due to the metabolic alterations noted below.

Gcgr$^{-/-}$ Mice Lack Functional Gcgrs. Liver membranes isolated from Gcgr$^{-/-}$ mice failed to bind [^{125}I]glucagon, whereas membranes from Gcgr$^{+/-}$ mice bound 59 ± 7.1% ($P < 0.01$, $n = 3$) of Gcgr$^{+/+}$ preparations (Fig. 1*a*). Accordingly, glucagon failed to stimulate cAMP production in Gcgr$^{-/-}$ membranes, whereas Gcgr$^{+/-}$ and Gcgr$^{+/+}$ generated similar increases in cAMP (Fig. 1*b*). Interestingly, basal cAMP levels in Gcgr$^{-/-}$ liver membranes were twice that of Gcgr$^{+/-}$ or Gcgr$^{+/+}$, whereas forskolin activation of adenylate cyclase stimulated similar cAMP production in all preparations. Finally, Gcgr$^{-/-}$ mice did not respond to glucagon challenge, whereas blood glucose (BG) levels of Gcgr$^{+/-}$ and Gcgr$^{+/+}$ mice increased to a peak of 10.5 ± 0.4 mM and 10.3 ± 0.7 mM, respectively (Fig. 1*c*). These data demonstrate Gcgr$^{-/-}$ mice lack functional Gcgrs, whereas Gcgr$^{+/-}$ mice display haploid insufficiency. The reduction in receptor number in Gcgr$^{+/-}$ mice does not appear to compromise glucagon stimulated glucose excursion in vivo and cAMP production *in vitro*.

Glucose Homeostasis in Gcgr$^{-/-}$ Mice. Glucagon is thought to be essential in maintaining fasting and postprandial glucose homeostasis, therefore glucose homeostasis was predicted to be

PHYSIOLOGY

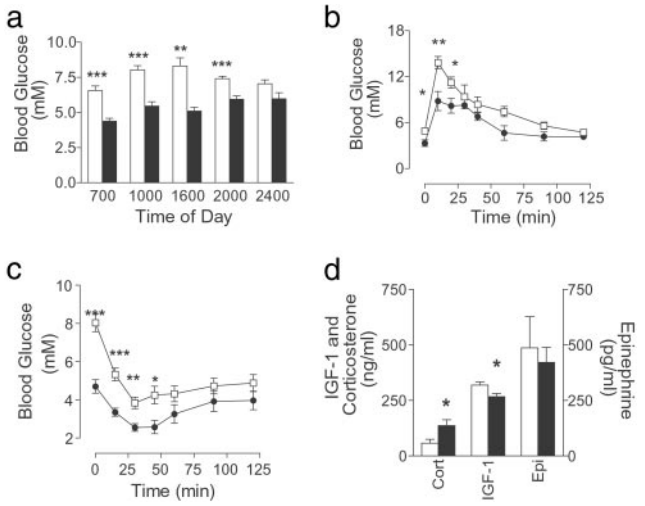

Fig. 2. Glucose homeostasis in Gcgr$^{-/-}$ mice. (*a*) BG levels throughout the day for 10- to 12-wk-old control and Gcgr$^{-/-}$ male mice. Gcgr$^{+/+}$, open bars; Gcgr$^{-/-}$, filled bars (n = 5–7). IPGTT (*b*) (n = 4–7) and ITT (*c*) (n = 5–7) of 17- to 19-wk-old male mice. Gcgr$^{+/+}$ mice (□) and Gcgr$^{-/-}$ mice (●) are indicated. (*d*) Fasted corticosterone (Cort) (n = 4), insulin-like growth factor-1 (n = 8), and epinephrine (Epi) (n = 8) serum levels in male Gcgr$^{+/+}$ (open bars) and Gcgr$^{-/-}$ (filled bars) mice. All data are mean ± SEM. *, $P < 0.05$; **, $P < 0.01$; ***, $P < 0.001$.

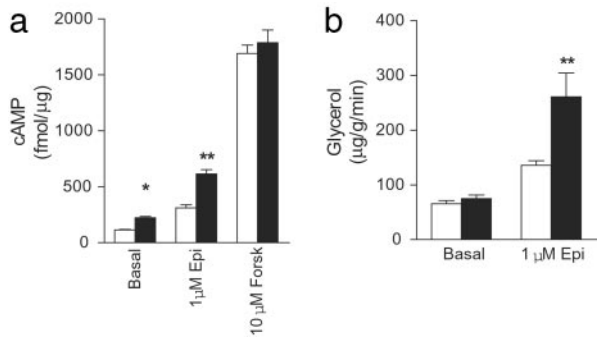

Fig. 3. Epinephrine-stimulated cAMP production in liver membranes and lipolysis in epididymal fat pads isolated from Gcgr$^{+/+}$ and Gcgr$^{-/-}$ mice. (*a*) Epinephrine (Epi)- and forskolin (Forsk)-stimulated cAMP production in Gcgr$^{+/+}$ (open bars) and Gcgr$^{-/-}$ (filled bars) mice. (*b*) Epinephrine-stimulated lipolysis as assessed by glycerol release. Data are representative of three experiments using three different membrane preparations. All data are the means ± SEM. *, $P < 0.05$; **, $P < 0.01$; ***, $P < 0.001$.

disrupted in Gcgr$^{-/-}$ mice. Gcgr$^{-/-}$ mice displayed significantly lower BG levels (daily average: Gcgr$^{-/-}$ males; 71.9 ± 2.4% of Gcgr$^{+/+}$, $P < 0.0001$, n = 5–7), except during peak feeding times (Fig. 2*a*). Similar reductions in BG were measured in mice at 22–24 wk (Table 1). When fasting was extended to 24 h, male Gcgr$^{-/-}$ mice developed severe hypoglycemia (Gcgr$^{-/-}$, 1.7 ± 0.1 mM vs. Gcgr$^{+/+}$, 3.7 ± 0.2 mM, $P < 0.01$, n = 6–8). These data indicate glucagon is essential for tight regulation of postprandial and fasting BG levels.

Similar insulin values were observed in Gcgr$^{-/-}$ and Gcgr$^{+/+}$ (Table 1). Impressively, ambient (2 h after lights were turned on) and fasting glucagon was 56- to 280-fold higher in Gcgr$^{-/-}$ mice compared with controls (Table 1). Conversely, serum leptin was 40–59% decreased in Gcgr$^{-/-}$ mice (Table 1). Fed, fasted, and/or ambient serum-free fatty acids, lactate, cholesterol, and high density lipoprotein were not significantly different in Gcgr$^{-/-}$ compared with Gcgr$^{+/+}$ mice (data not shown). Although fasting triglycerides (TG) in Gcgr$^{-/-}$ mice were similar to Gcgr$^{+/+}$ mice, ambient TG levels were 60% decreased in female Gcgr$^{-/-}$ mice (Table 3, which is published as supporting information on the PNAS web site). In addition, fed and ambient plasma low density lipoprotein was increased 1.6- to 3.3-fold in Gcgr$^{-/-}$ mice.

IPGTT (Fig. 2*b*) showed a significant reduction in the area under the curve (male Gcgr$^{-/-}$; 676 ± 38 vs. male Gcgr$^{+/+}$, 911 ± 51 mM/120 min, $P < 0.0001$, n = 5–7) in Gcgr$^{-/-}$ mice, indicating improved glucose tolerance. In ITT (Fig. 2*c*), Gcgr$^{-/-}$ mouse BG levels decreased to levels lower than that seen for controls, although relative change from basal levels were similar (Gcgr$^{-/-}$; 59 ± 10 vs. male Gcgr$^{+/+}$, 49 ± 6% of BG at time 0). Interestingly, despite the lack of glucagon action, BG of Gcgr$^{-/-}$ mice was restored to control levels by 60 min.

Because Gcgr$^{-/-}$ mice were able to compensate in part for loss of glucagon action, fasting (12–14 h) levels of compensatory hormones such as epinephrine, insulin-like growth factor-1 (IGF-1) (to reflect circadian growth hormone release), and corticosterone, which regulate HGP, were examined (Fig. 2*d*). Although epinephrine levels were similar to controls, there was a small decrease in IGF-1 and a 2-fold increase in corticosterone in fasting Gcgr$^{-/-}$ mice (Fig. 2*d*). However, afternoon corticosterone levels of female Gcgr$^{-/-}$ mice were lower than controls (female Gcgr$^{-/-}$, 422 ± 22 vs. female Gcgr$^{+/+}$, 530 ± 16 pg/ml, $P < 0.01$, n = 10), suggesting corticosterone release was normal under basal conditions in Gcgr$^{-/-}$ mice, and that the prolonged hypoglycemia experienced by Gcgr$^{-/-}$ compared with control animals was responsible for the increased levels observed during a fast. To examine whether increased responsiveness to counterregulatory hormones partially compensates for loss of glucagon action, epinephrine-stimulated cAMP production by liver membrane preparations and lipolysis in WAT were measured (Fig. 3). Both basal and epinephrine (1 μM) stimulated cAMP levels in Gcgr$^{-/-}$ liver membranes were twice that of controls, indicating increased responsiveness to epinephrine. Although basal lipolysis in WAT, assessed by glycerol release, was similar in

Table 1. Male serum hormone and metabolite levels in the fasted, fed, or ambient states

	Gcgr$^{+/+}$		Gcgr$^{-/-}$	
	Fasted	Fed	Fasted	Fed
Glucose, mM	6.6 ± 0.4	6.9 ± 0.4	4.2 ± 0.3**	5.5 ± 0.3*
Insulin, ng/ml	0.99 ± 0.18	1.71 ± 0.23	0.89 ± 0.10	1.33 ± 0.25
Glucagon, pg/ml†	45 ± 8	63 ± 7	12,708 ± 1,759***	4,621 ± 542***
Leptin, ng/ml†	9.3 ± 1.1	ND	3.8 ± 0.7**	ND
TG, mM†	0.82 ± 0.20	1.91 ± 0.20	0.70 ± 0.21	1.09 ± 0.34
LDL, mM†	0.08 ± 0.02	0.11 ± 0.03	0.27 ± 0.04***	0.28 ± 0.03**

Data are the mean ± SEM, n = 5–7. *, $P < 0.05$; **, $P < 0.01$; ***, $P < 0.001$.
†Ambient plasma levels were determined.

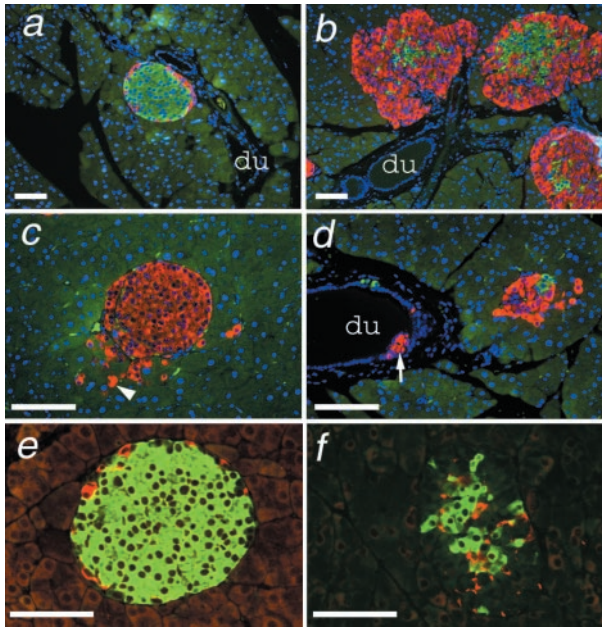

Fig. 4. Gcgr$^{-/-}$ mice have islet and α cell hyperplasia. Photomicrographs of pancreatic sections from Gcgr$^{+/+}$ (*a* and *e*) and Gcgr$^{-/-}$ (*b–d* and *f*) mice double immunostained for insulin (green) and glucagon (red), with nuclei visualized by Hoechst staining in blue (*a–d*) or insulin (green) and somatostatin (red) (*e* and *f*). du, ductal epithelium in *a–c*. In *c*, the arrowhead indicates single glucagon-positive cells within exocrine tissue adjacent to an islet. Arrowhead in *d* indicates an accumulation of glucagon-positive cells within the ductal epithelium. Pancreata were from female mice 8–9 wk of age (*a* and *b*) and 18 wk of age (*c* and *d*). Pancreata in *e* and *f* were from 18- to 20-wk-old male mice. Bars indicate 100 μm.

Gcgr$^{-/-}$ and Gcgr$^{+/+}$ mice, 1 μM epinephrine stimulated a 66% increase in glycerol release in Gcgr$^{-/-}$ preparations.

Gcgr$^{-/-}$ Mice Have Pancreatic Endocrine Hyperplasia. The most striking effect of the Gcgr$^{-/-}$ mutation was an extreme hypertrophy of the pancreas. Pancreata from Gcgr$^{-/-}$ mice as young as 6 wk of age weighed 2- to 3.5-fold more than Gcgr$^{+/+}$ mice (Fig. 5*a*). Double immunofluorescence labeling indicated an overall hyperplasia of Gcgr$^{-/-}$ islets, with a predominant hyperplasia of the α cell mantle (Fig. 4 *b–d*). Interestingly, islets were often clustered near ductal tissue (Fig. 4 *b–d*), and glucagon staining was seen along and budding from ductal epithelium (Fig. 4*d*) or within exocrine tissue (Fig. 4*c*). Ductal staining appeared to be increased in older animals (Fig. 4 *c* and *d*). Islets of Gcgr$^{-/-}$ mice had densely staining core regions of insulin-positive cells (Fig. 4 *b* and *f*). Somatostatin staining appeared to be increased in Gcgr$^{-/-}$ islets and was restricted to the inner layer of the expanded α cell mantle or scattered randomly throughout the islet cell mass (Fig. 4*f*). No gross morphological differences were observed in the exocrine tissue (Fig. 9, which is published as supporting information on the PNAS web site). Interestingly, pancreata of 1-day-old Gcgr$^{-/-}$ and Gcgr$^{+/+}$ pups did not display any gross differences in size or islet cell distribution (data not shown), indicating postnatal hyperplasia of the Gcgr$^{-/-}$ endocrine pancreas.

Pancreata were extracted and assayed for specific islet hormone content (Table 2). As predicted, an antibody detecting both glucagon and proglucagon indicated a 9-fold increase in total pancreatic glucagon in Gcgr$^{-/-}$ mice. Although insulin content of Gcgr$^{-/-}$ mice pancreata did not differ from controls, somatostatin levels were increased 4-fold (Table 2), supporting a contribution by δ cells to the islet hyperplasia. Because small amounts of proglucagon are normally processed to GLP-1 (1–37 and 1–36 amide) in the pancreas (21), pancreatic content of these polypeptides was examined by using antibodies specific for all processed forms of GLP-1 (total = 1–36 amide, 7–36 amide, 1–37, and 7–37) and another for all amidated forms of GLP-1 (Table 2). The content of total and amidated GLP-1 in Gcgr$^{-/-}$ pancreas extracts was increased 25 and 10 times, respectively. The altered processing was associated with 3- to 10-fold higher circulating GLP-1 amide levels in Gcgr$^{-/-}$ mice (males, Gcgr$^{+/+}$, 21 ± 2 vs. Gcgr$^{-/-}$, 79 ± 8 pM, n = 6–9, $P <$ 0.0001; females, Gcgr$^{+/+}$, 16 ± 1 vs. Gcgr$^{-/-}$, 167 ± 28 pM, $P <$ 0.0001, n = 9–10). The source of circulating GLP-1 amide appeared to be the pancreas, because intestinal extracts from female Gcgr$^{-/-}$ and control mice were similar (total GLP-1; Gcgr$^{+/+}$, 281 ± 125 vs. Gcgr$^{-/-}$, 207 ± 99 pmol/g, n = 5; amidated GLP-1; Gcgr$^{+/+}$, 46.4 ± 14.5 vs. Gcgr$^{-/-}$, 42.2 ± 15.8 pmol/g, n = 5).

Table 2. Pancreatic tissue concentration of islet hormones in male mice, 14–22 wk

Hormone	Gcgr$^{+/+}$	Gcgr$^{-/-}$
Insulin	8,387 ± 814	6,391 ± 961
Somatostatin	1,452 ± 451	4,270 ± 1,021*
Glucagon + ProGlu	542 ± 125	4,933 ± 1,450**
GLP-l amide	25 ± 2	233 ± 35***
Total GLP-1	63 ± 8	1,633 ± 427**

Concentrations are in fmol/mg. Data are the mean ± SEM, n = 11–12. *, $P <$ 0.05; **, $P <$ 0.01; ***, $P <$ 0.001.

Other organs that express Gcgr were examined to determine whether loss of Gcgr function resulted in other gross morphological differences in Gcgr$^{-/-}$ mice (Fig. 5*a*). Male Gcgr$^{-/-}$ liver weights were similar to control mice. Because loss of glucagon action could lead to decreased glycogenolysis, hepatic glycogen content was measured. Ambient hepatic glycogen levels in Gcgr$^{-/-}$ mice were increased by 65% (males; Gcgr$^{-/-}$, 165 ±

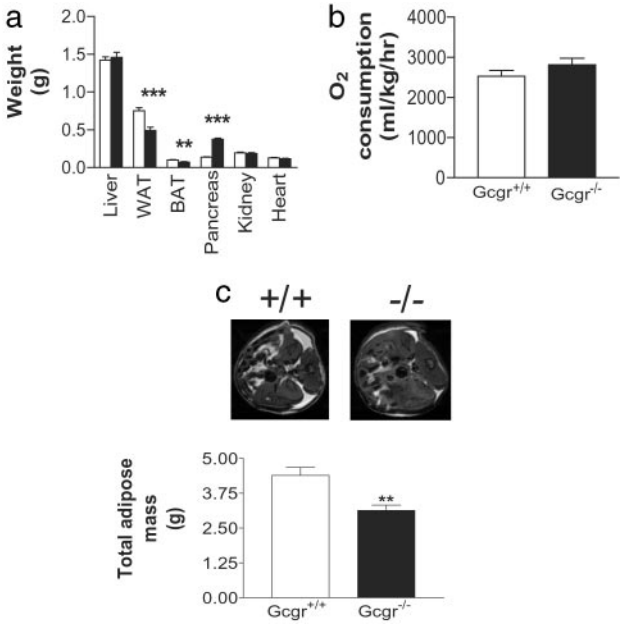

Fig. 5. (*a*) Comparison of organ weights from 22- to 24-wk-old Gcgr$^{+/+}$ and Gcgr$^{-/-}$ male mice (n = 5–14). Control (open bars) and Gcgr$^{-/-}$ (filled bars) mice are shown. WAT, perigonadal WAT; BAT, interscapular brown adipose tissue. (*b*) Indirect calorimetry measurements of O_2 consumption. Resting VO_2 values were determined for male mice 23–25 wk of age (n = 4). (*c*) MRI analysis of male Gcgr$^{-/-}$ mice. (*Upper*) Abdominal MRI images of Gcgr$^{+/+}$ and Gcgr$^{-/-}$ mice. Adipose tissue appears white. (*Lower*) Comparison of total body adipose tissue (n = 5). All data are mean ± SEM. *, $P <$ 0.05; **, $P <$ 0.01; ***, $P <$ 0.001.

PHYSIOLOGY

12% of control, $P < 0.01$, $n = 5–6$), suggesting Gcgr$^{-/-}$ mice do not mobilize glycogen as efficiently as Gcgr$^{+/+}$ mice in the initial postprandial state. In the fasting state, glycogen levels in Gcgr$^{-/-}$ compared with Gcgr$^{+/+}$ mice were not significantly different (males; Gcgr$^{-/-}$, 150 ± 25% control, $n = 5–6$).

Gcgr$^{-/-}$ Mice Display a Lean Phenotype. As predicted by the lower serum leptin of Gcgr$^{-/-}$ mice, the weight of perigonadal WAT was decreased in Gcgr$^{-/-}$ mice (Fig. 5*a*). In addition, a smaller yet significant decrease in interscapular brown fat pad weight was noted. Because Gcgr$^{-/-}$ and Gcgr$^{+/+}$ mice displayed similar growth rates (Fig. 7) and cumulative food intake (males, Gcgr$^{+/+}$, 263.6 ± 4.5 vs. Gcgr$^{-/-}$, 265.7 ± 4.6 g/mouse/5 wk, $n = 3$), an increase in lean body mass was predicted. MRI revealed a 1.3-g decrease in total body adipose mass (Fig. 5*c*) in Gcgr$^{-/-}$ mice corresponding to a 10% reduction in adipose mass as a ratio of total body mass. This decrease in adipose mass, but nominal total body mass, indicated Gcgr$^{-/-}$ mice had a 10% increase in lean body mass (Table 4, which is published as supporting information on the PNAS web site). In agreement with the similarity in growth rate and food intake, indirect calorimetry of male mice 11–12 wk of age showed similar resting O_2 consumption (Fig. 5*b*) and energy expenditure (Gcgr$^{+/+}$, 0.37 ± 0.02 vs. Gcgr$^{-/-}$, 0.37 ± 0.03 kcal/hr, $n = 4$).

Discussion

Glucagon has long been thought to be the primary counterregulatory hormone to insulin, preventing hypoglycemia by increasing HGP (1, 2). Our finding that targeted disruption of the *Gcgr* gene results in lower BG throughout the day and in the fasting state supports such a role for glucagon in the maintenance of homeostatic glucose levels. There have been two other brief reports on Gcgr$^{-/-}$ mice (22, 23). Similar to what is reported here, both groups found that Gcgr$^{-/-}$ mice appeared normal, reached normal body weight, and had normal plasma insulin, but displayed elevated glucagon levels. The present study further describes the alterations in glucose homeostasis and glycogen metabolism, islet morphology, and pancreatic hormone content and release, as well as identifies alterations in the adiposity of Gcgr$^{-/-}$ mice.

The most distinguishing change observed in Gcgr$^{-/-}$ mice was the massive enlargement of the pancreas, which involved at least in part a predominate α cell hyperplasia, associated with supraphysiological levels of glucagon. In addition, although it remains to be quantitatively determined, there appears to be a concomitant hypertrophy of the exocrine cell mass. Although Parker and colleagues noted elevated fasting and fed glucagon levels in Gcgr$^{-/-}$ mice, they also noted a significant increase in glucagon levels in Gcgr$^{+/+}$ mice (23), which was not observed in either of the two lines generated here. Parker *et al*. (23) suggested that the genetic manipulation may have reduced receptor expression in some way, implying a secondary genetic integration or random mutation event occurred that could complicate interpretation of their model.

We recently identified an individual carrying a homozygous point mutation in the *Gcgr* gene that results in ablation of receptor activity (L. H. Hansen, E. Larger, R.W.G., J.-C. Chaput, C. Vissuzaine, J. Capeau, C. Deacon, J.J.H., O. D. Madsen, F. Yakushiji, *et al*., unpublished results). The almost identical hyperplasia of the pancreas and α cell mass of this individual to the Gcgr$^{-/-}$ mouse indicates glucagon signaling via its receptor is important for normal pancreatic endocrine and possibly exocrine cell proliferation in humans as well as mice. In addition, mice deficient in prohormone convertase 2 (PC2), which lack mature glucagon due to defective proglucagon processing, display a similar reduction in BG, islet α and δ cell hyperplasia (24), and similar shallow glucose tolerance curves (25). However, these mice also have defects in processing many islet hormones (24, 26) and neuropeptides (27). Interestingly, loss of glucagon action in Gcgr$^{-/-}$ and PC2$^{-/-}$ mice resulted in islet hyperplasia and α cell proliferation. Further, Gcgr$^{-/-}$ mice displayed an enlarged pancreas and normal insulin levels, whereas PC2$^{-/-}$ mice had no hyperplasia of the pancreas and reduced insulin levels (25), indicating differences in the phenotypes exist.

Importantly, Gcgr$^{-/-}$ mice had clusters of islets near ducts, with glucagon-positive staining often seen lining and budding from ductal regions where pluripotent progenitor cells for endocrine cell lineages are thought to reside (28, 29). These findings suggest that lack of glucagon signaling may initiate proliferation of pluripotent progenitor endocrine cells within ductal epithelium (28, 29), either directly or via the release of growth factors and activation of transcription factors involved in development of the endocrine pancreas (30). Given that pancreas size and islet morphology appeared normal in 1-day-old Gcgr$^{-/-}$ mice, and ductal staining was seen in adult Gcgr$^{-/-}$ mice, it appears that lack of glucagon signaling can initiate differentiation of pluripotent progenitor endocrine cells into glucagon-producing cells postnatally. That glucagon may in fact be the signaling molecule is supported by the observation that replacement of glucagon via osmotic micropump corrected both BG level and the α cell hyperplasia of prohormone convertase 2$^{-/-}$ mice (31). However, because both glucagon and glucose levels were restored, it remains unclear whether glucagon alone or euglycemia itself was responsible for correction of the hyperplasia. Replacement of the Gcgr in a tissue-specific manner by crossing Gcgr$^{-/-}$ mice with tissue-specific Gcgr transgenic mice may help to identify which Gcgr-expressing tissues are responsible for the α and δ cell hyperplasia.

Prohormone processing of proglucagon in the pancreas usually leads to formation of small amounts (<2% of proglucagon) of GLP-1, mostly in the form of GLP-1 1–37 and 1–36 amide (21). Overproduction of proglucagon in Gcgr$^{-/-}$ mice resulted in altered processing of the C terminus of proglucagon, as indicated by increased pancreatic content of GLP-1 (33% of proglucagon) and GLP-1 amide (5% of proglucagon) in Gcgr$^{-/-}$ mice. Although the assays used did not differentiate between pancreatic and intestinally processed GLP-1 (GLP-1 7–36 amide and 7–27), the GLP-1 content of intestinal extracts of Gcgr$^{-/-}$ mice did not differ from control animals, suggesting that the increased circulating GLP-1 amide observed in Gcgr$^{-/-}$ mice originates from the pancreas. Although the physiological role of N-terminally extended forms of GLP-1 remains largely unknown, it is well established that intestinally processed forms of GLP-1 (7–36 amide and 7–27) act to increase insulin secretion, β cell glucose sensitivity, and β cell mass, as well as inhibit glucagon secretion and inhibit food intake via the CNS. Because both N-terminally extended GLP-1 and glucagon can bind and activate the GLP-1 receptor with reduced affinity and efficacy (32), to what extent this may contribute, if at all, to the Gcgr$^{-/-}$ phenotype remains to be determined. Generation of mice lacking both the GLP-1 receptor (GLP-1R) and Gcgr will allow the contribution of the elevated GLP-1 to the Gcgr$^{-/-}$ phenotype to be determined.

Gcgr$^{-/-}$ mice displayed lower glucose levels during ITT, although the relative changes in glucose levels were similar, suggesting insulin sensitivity was similar to control animals, although glycemic clamp studies need to be carried out to definitively determine whether insulin sensitivity is altered in Gcgr$^{-/-}$ mice. In contrast, Gcgr$^{-/-}$ mice displayed shallow IPGTT curves compared with control mice. Interestingly, despite lower BG levels, insulin levels in the fasted and fed state were similar in Gcgr$^{-/-}$ and control mice, suggesting that glucose-stimulated insulin release was increased in Gcgr$^{-/-}$. Given that GLP-1 has been shown to be important to the regulation of fasting and nonenteral glucose clearance (33), the increased GLP-1 levels observed in Gcgr$^{-/-}$ may account for the apparent enhancement of glucose-stimulated insulin secretion and glucose tolerance. Alternatively, protein kinase A (PKA) and C (PKC) serine/threonine phosphorylation of the insulin receptor (34, 35) and downstream mediators of insulin action, insulin receptor substrate (IRS)-1 and -2 (36, 37), has been

shown to reduce tyrosine phosphorylation and signaling through this pathway. It may be that glucagon and its receptor counterregulate insulin action in peripheral tissues and liver via activation of PKA and/or PKC. Loss of this counterregulation along with normal insulin levels could account for improved glucose tolerance in $Gcgr^{-/-}$ mice. In support of this hypothesis, mice heterozygous for a null deletion of the GTP-binding protein, $G_{s\alpha}$, a G protein the Gcgr likely couples to, have increased insulin sensitivity and display improved glucose tolerance (38).

In addition to glucagon, there are other hormonal, nutrient/fuel, and neural regulators of HGP that protect against hypoglycemia. That $Gcgr^{-/-}$ BG levels returned to control levels within 60 min of insulin injection indicated compensatory mechanisms still function in $Gcgr^{-/-}$ mice. Of the counterregulatory hormones examined, only corticosterone levels were increased during a fast. However, because late afternoon levels of corticosterone did not differ between $Gcgr^{-/-}$ and controls, increased corticosterone release does not appear to be a general compensatory mechanism. Epinephrine (1 μM) stimulated cAMP production by liver membranes, and lipolysis from WAT was increased, 97% and 66%, respectively, in $Gcgr^{-/-}$ compared with control mice. Interestingly, basal lipolysis was similar in $Gcgr^{-/-}$ and $Gcgr^{+/+}$ WAT, whereas basal cAMP production in $Gcgr^{-/-}$ liver membranes was twice that of controls. These data suggest $Gcgr^{-/-}$ mice may compensate for loss of glucagon action in part by increased basal signaling in liver and increased responsiveness to epinephrine in liver and WAT. It remains to be determined whether sensitivity to other compensatory hormones is increased, and what molecular mechanisms are responsible for the observed increase in epinephrine signaling.

A perplexing observation in $Gcgr^{-/-}$ mice was the lean phenotype with lower leptin levels, despite having normal growth rates, body weight (Fig. 8), food intake, and resting energy expenditure. The decrease in fat mass was indeed matched by a similar increase in lean body mass. Because regulation of energy balance is mainly mediated centrally (4), it is possible that the loss of glucagon action or the increased GLP-1 signaling in the CNS may play a role in this change in body composition, perhaps via increased sensitivity to leptin. Alternatively, loss of glucagon action or increased GLP-1 signaling in peripheral tissues may result in a change in body composition. However, the mechanism by which fat mass is decreased and lean body mass is increased in this animal model remains to be determined.

In conclusion, we provide a detailed characterization of mice engineered with a Gcgr null mutation. Our findings demonstrate glucagon plays an important role in regulation of pancreas and islet cell mass, particularly that of the α and δ cells. Importantly, $Gcgr^{-/-}$ mice displayed chronically lower BG levels despite increased sensitivity to other counterregulatory hormones, underscoring the importance of glucagon action in glucose homeostasis. In addition, $Gcgr^{-/-}$ mice displayed altered adiposity, raising the possibility that glucagon and its receptor, directly or via regulation of another factor, may play an essential role in regulation of body composition. Thus, $Gcgr^{-/-}$ mice should prove useful for studies into the regulation of glucagon secretion, identification of factors involved in pancreatic proliferation, and hepatic counterregulatory mechanisms, as well as regulation of whole body composition. In addition, because hyperglucagonemia and increased basal HGP are characteristics of type II diabetes (1, 39, 40), induction of a diabetic state in $Gcgr^{-/-}$ mice will provide an invaluable model for determining the contribution of glucagon to hyperglycemia.

The expert technical assistance of R. M. Ingvorsen, S. Primdahl, A. T. Christensen, and K. Geisler Heding is gratefully acknowledged. We also thank J. Nowak and J. Hummeluhr Rasmussen for assistance with general histology. We thank Drs. E. B. Katz, J. Li, R. Burcelin, and M. W. Schwartz for thoughtful discussions and advice on the manuscript. This work was supported by the National Institutes of Health (Grants DK47425 and HL58119), the American Diabetes Association, Albert Einstein College of Medicine (AECOM) Comprehensive Cancer Center (to M.J.C.), the AECOM Diabetes Center (to M.J.C. and L.R.), and the Danish Medical Research Council (to J.J.H.). M.J.C. is an Irma T. Hirschl Career Scientist.

1. Burcelin, R., Katz, E. B. & Charron, M. J. (1996) *Diabetes Metab.* **22,** 373–396.
2. Lefèbvre, P. J. (1995) *Diabetes Care* **18,** 715–730.
3. Kieffer, T. J. & Habener, J. F. (1999) *Endocr. Rev*. **20,** 876–913.
4. Porte, D., Jr., Seeley, R. J., Woods, S. C., Baskin, D. G., Figlewicz, D. P. & Schwartz, M. W. (1998) *Diabetologia* **41,** 863–881.
5. Holst, J. J. (2000) *Regul. Pept.* **93,** 45–51.
6. Drucker, D. J. (2001) *Endocrinology* **142,** 521–527.
7. Jelinek, L. J., Lok, S., Rosenberg, G. B., Smith, R. A., Grant, F. J., Biggs, S., Bensch, P. A., Kuijper, J. L., Sheppard, P. O. & Sprecher, C. A. (1993) *Science* **259,** 1614–1616.
8. Lok, S., Kuijper, J. L., Jelinek, L. J., Kramer, J. M., Whitmore, T. E., Sprecher, C. A., Mathewes, S., Grant, F. J., Biggs, S. H. & Rosenberg, G. B. (1994) *Gene* **140,** 203–209.
9. Burcelin, R., Li, J. & Charron, M. J. (1995) *Gene* **164,** 305–310.
10. Ulrich, C. D., Holtmann, M. & Miller, L. J. (1998) *Gastroenterology* **114,** 382–397.
11. Katz, E. B., Stenbit, A. E., Hatton, K., DePinho, R. & Charron, M. J. (1995) *Nature* **377,** 151–155.
12. Nishimura, E., Billestrup, N., Perrin, M. & Vale, W. (1987) *J. Biol. Chem*. **262,** 12893–12896.
13. Madsen, P., Knudsen, L. B., Wiberg, F. C. & Carr, R. D. (1998) *J. Med. Chem.* **41,** 5150–5157.
14. Katz, J., Golden, S. & Wals, P. A. (1976) *Proc. Natl. Acad. Sci. USA* **73,** 3433–3437.
15. Fosgerau, K., Westergaard, N., Quistorff, B., Grunnet, N., Kristiansen, M. & Lundgren, K. (2000) *Arch. Biochem. Biophys*. **380,** 274–284.
16. Dolnikoff, M., Martin-Hidalgo, A., Machado, U. F., Lima, F. B. & Herrera, E. (2001) *Int. J. Obes. Relat. Metab. Disord*. **25,** 426–433.
17. Friis-Hansen, L., Lacourse, K. A., Samuelson, L. C. & Holst, J. J. (2001) *J. Endocrinol.* **169,** 595–602.
18. Stein, D. T., Babcock, E. E., Malloy, C. R. & McGarry, J. D. (1995) *Int. J. Obes. Relat. Metab. Disord*. **19,** 804–810.
19. Jensen, J., Serup, P., Karlsen, C., Nielsen, T. F. & Madsen, O. D. (1996) *J. Biol. Chem*. **271,** 18749–18758.
20. Blume, N., Skouv, J., Larsson, L.-I., Holst, J. J. & Madsen, O. D. (1995) *J. Clin. Invest.* **96,** 2227–2235.
21. Holst, J. J., Bersani, M., Johnsen, A. H., Kofod, H., Hartmann, B. & Ørskov, C. (1994) *J. Biol. Chem.* **269,** 18827–18833.
22. Amatruda, J. & Livingston, J. (1996) in *Handbook of Experimental Pharmacology*, ed. Lefèbvre, P. J. (Springer, Berlin), pp. 133–147.
23. Parker, J. C., Andrews, K. M., Allen, M. R., Stock, J. L. & McNeish, J. D. (2002) *Biochem. Biophys. Res. Commun*. **290,** 839–843.
24. Wang, J., Xu, J., Finnerty, J., Furuta, M., Steiner, D. F. & Verchere, C. B. (2001) *Diabetes* **50,** 534–539.
25. Furuta, M., Yano, H., Zhou, A., Rouille, Y., Holst, J. J., Carroll, R., Ravazzola, M., Orci, L., Furuta, H. & Steiner, D. F. (1997) *Proc. Natl. Acad. Sci. USA* **94,** 6646–6651.
26. Furuta, M., Carroll, R., Martin, S., Swift, H. H., Ravazzola, M., Orci, L. & Steiner, D. F. (1998) *J. Biol. Chem*. **273,** 3431–3437.
27. Zhou, A., Webb, G., Zhu, X. & Steiner, D. F. (1999) *J. Biol. Chem*. **274,** 20745–20748.
28. Rall, L. B., Pictet, R. L., Williams, R. H. & Rutter, W. J. (1973) *Proc. Natl. Acad. Sci. USA* **70,** 3478–3482.
29. Bouwens, L. & Blay, E. D. (1996) *J. Histochem. Cytochem*. **44,** 947–951.
30. Nielsen, J. H. & Serup, P. (1998) *Curr. Opin. Endocrinol. Diabetes* **5,** 97–107.
31. Webb, G. C., Akbar, M. S., Zhao, C., Swift, H. H. & Steiner, D. F. (2002) *Diabetes* **51,** 398–405.
32. Creutzfeldt, W. & Ebert, R. (1993) in *The Pancreas: Biology, Pathobiology, and Disease*, eds. Lang, V. & Go, I. (Raven, New York), pp. 769–788.
33. Baggio, L., Kieffer, T. J. & Drucker, D. J. (2000) *Endocrinology* **141,** 3703–3709.
34. Stadtmauer, L. & Rosen, O. M. (1986) *J. Biol. Chem*. **261,** 3402–3407.
35. Takayama, S., White, M. F. & Kahn, C. R. (1988) *J. Biol. Chem*. **263,** 3440–3447.
36. Le Roith, D. & Zick, Y. (2001) *Diabetes Care* **24,** 588–597.
37. Paz, K., Hemi, R., LeRoith, D., Karasik, A., Elhanany, E., Kanety, H. & Zick, Y. (1997) *J. Biol. Chem.* **272,** 29911–29918.
38. Yu, S., Castle, A., Chen, M., Lee, R., Takeda, K. & Weinstein, L. S. (2001) *J. Biol. Chem.* **276,** 19994–19998.
39. Brand, C. L., Jorgensen, P. N., Svendsen, I. & Holst, J. J. (1996) *Diabetes* **45,** 1076–1083.
40. Brand, C. L., Rolin, B., Jorgensen, P. N., Svendsen, I., Kristensen, J. S. & Holst, J. J. (1994) *Diabetologia* **37,** 985–993.